

# PCN224 Mediated Sono-Photodynamic Therapy Triggers Apoptosis through Multisite Damage in Hepa1-6 Cells

Jingsong Cui<sup>1,†</sup>, Haiping Wang<sup>2,†</sup>, Fang Yang<sup>2</sup>, Qian Peng<sup>1</sup>, Weiling Li<sup>2</sup>, Kanghong Hu<sup>1,\*</sup>, Binlian Sun<sup>2,\*</sup>

<sup>1</sup>Sino-German Biomedical Center, National “111” Center for Cellular Regulation and Molecular Pharmaceutics, Cooperative Innovation Center of Industrial Fermentation (Ministry of Education & Hubei Province), Hubei University of Technology, 430068 Wuhan, Hubei, China

<sup>2</sup>Wuhan Institute of Biomedical Sciences, School of Medicine, Jiangnan University, 430056 Wuhan, Hubei, China

\*Correspondence: [hukh@hbut.edu.cn](mailto:hukh@hbut.edu.cn) (Kanghong Hu); [binlian17@jhun.edu.cn](mailto:binlian17@jhun.edu.cn) (Binlian Sun)

†These authors contributed equally.

Published: 20 April 2023

**Background:** Sono-photodynamic therapy (SPDT) is a novel anti-cancer strategy that has showed excellent preclinical anti-tumor effects by combining the advantage of photodynamic and sonodynamic therapy. Sensitizer is the most important element in SPDT, which directly influences the cytotoxicity of SPDT. This study investigated the effect of using sensitizer PCN 224 (PCN224-SPDT) in SPDT on mouse hepatocellular carcinoma Hepa1-6 (mouse hepatoma cells).

**Methods:** Hepa1-6 cells were divided into a control group, PCN224 alone group (PCN224), ultrasound treatment alone group (US), PDT (photodynamic therapy) group (PCN224 + 5 J/cm<sup>2</sup> laser), SDT (sonodynamic therapy) group (PCN224 + 1 W/cm<sup>2</sup> ultrasound) and SPDT group (PCN224 + 5 J/cm<sup>2</sup> laser + 1 W/cm<sup>2</sup> ultrasound). The 3-(4,5-dimethylthiazol-2-yl)-2,5-diphenyltetrazole ammonium bromide (MTT) was used to detect cytotoxicity. The uptake and distribution of PCN224 in Hepa1-6 cells were determined by fluorescence staining. Flow cytometry was used to analyze intracellular reactive oxygen species (ROS) levels, cell membrane permeability, DNA damage, cell apoptosis levels, and mitochondrial membrane potential. Scanning transmission electron microscopy (SEM) was used to observe the changes in cell microstructure.

**Results:** PCN224-SPDT induced severe damage to the cell membrane, mitochondrial and deoxyribonucleic acid (DNA), ultimately resulting in cell apoptosis.

**Conclusions:** This work suggests that PCN224 is a new sensitizer for SPDT, and PCN224-SPDT can cause Hepa1-6 cells multisite damage and induce cell apoptosis via ROS production.

**Keywords:** sono-photodynamic; PCN224; reactive oxygen species; multisite damage; apoptosis

## Introduction

Photodynamic therapy (PDT) is a kind of physical modality used in the clinical treatment of superficial tumors [1,2]. Compared with traditional strategies, such as surgery, chemotherapy and radiotherapy, PDT can eliminate tumor cells without severe side effects. Photosensitizers, laser light and oxygen are the three important elements in PDT. In PDT, photosensitizers absorb energy from laser light, which is transferred to oxygen to produce reactive oxygen species (ROS), and then the ROS plays cytotoxic to tumor cells [3,4]. Furthermore, the preferential enrichment of some photosensitizers in tumor tissues due to the rapid proliferation of tumor cells and the property of photosensitizers, and the local site light irradiation can reduce the off-target toxicity to surrounding tissues [5]. Furthermore, numerous studies have showed that PDT can combine with other therapeutic modalities and cause synergetic effects [6]. However, the poor penetration of laser light dramatically limits the application of PDT in deep-site tumors [7].

Unlike laser light, ultrasound can penetrate deep tissue (about 8~10 cm) [8] as a readily available, inexpensive and non-invasive method. Ultrasound has been widely used as a diagnostic tool, drug delivery and anti-tumor therapy [9]. In addition, the combination of ultrasound and sonosensitizers called sonodynamic therapy (SDT) has emerged as a promising anti-cancer modality since its development in the late 1980s. In SDT treatment, ultrasound is used to activate sensitizers to generate cytotoxic ROS. As PDT has a high penetration of ultrasound, it can target on deep-site tumors and activate sonosensitizers in tumor cells, achieving tumor suppression or clearance [10]. Because most sensitizers can be activated by light and ultrasound, the combination of SDT and PDT (sono-photodynamic therapy, SPDT) is used for anti-tumor research. SPDT showed a synergetic anti-tumor effect by enhancing cellular ROS production and cell apoptosis [11].

Many sensitizers have been used in SPDT treatment, such as Chlorin e6, Sinoporphyrin sodium, sonnelux, and

chlorophyll [12–14]. Seeking novel photo/sonosensitizers is vital for SPDT treatment in anti-tumor fields. PCN224 is nanoparticles showing high photo-oxygenation efficiency, good biocompatibility, and high stability, and it is a kind of porphyrin-based Metal-organic frameworks (MOFs) using porphyrins (TCPP) as organic linkers to form MOFs [15] to combine the advantages of porphyrins and MOFs. Moreover, the nanoscale PCN224 has been used in drug delivery, bioimaging, and tumor therapy [16]. The high porphyrin loading capacity, free diffusion of oxygen and singlet oxygen in the pores of PCN224 make it efficient photosensitizers [17]. However, whether PCN224 can also be activated by ultrasound has never been reported. In this study, we aim to use PCN224 in the SPDT and investigate the effects of PCN224-SPDT on the mouse liver cancer Hepa1-6 cells *in vitro*.

## Materials and Methods

### Materials

PCN224 (R-PN1009) was purchased from Xi'an Ruixi Biological Technology Co., Ltd. (Xi'an, China). The 3-(4,5-dimethyl-2-thiazolyl)-2,5-diphenyl-2-H-tetrazolium bromide (MTT, 298-93-1), N-acetylcysteine (NAC, 38520-57-9) paraformaldehyde, glutaraldehyde (111-30-8) and propidium iodide (PI, 25535-16-4) were obtained from Sigma Chemical Company (Darmstadt, Germany). The 2',7'-Dichlorofluorescein diacetate (DCFH-DA, 2044-85-1) and Hoechst 33342 (HO, 875756-97-1) were purchased from Molecular Probes Inc. (Eugene, OR, USA). Tetramethylrhodamine methyl ester (115532-50-8) was purchased from Thermo Fisher Scientific (Waltham, MA, USA). Dimethyl sulfoxide (67-68-5) was obtained from Shanghai Aladdin Biochemical Technology Co., Ltd. (Shanghai, China).

### Cell Lines

Hepa1-6 (Mouse hepatoma cells) cells were purchased from ATCC (American type culture collection, Rockefeller, MD, USA) and cultured in the Dulbecco's Modified Eagle Medium (DMEM, 12430054, Gibco, New York, NY, USA) supplemented with 10% fetal bovine serum (FBS, 10099-141, Gibco, New York, NY, USA) and 1% antibiotics at 37 °C in a humidified atmosphere of 5% CO<sub>2</sub>. The PCR (Polymerase Chain Reaction) method for detection of mycoplasma in cells was free of mycoplasma contamination, and the cell lines were identified by the STR (Short Tandem Repeat) method.

Cells were cultured in T25 culture flasks and passaged when the cells covered about 70%–80% of the bottom of the flask. We discarded the original medium, washed twice with PBS (phosphate buffered solution) and added 1 mL of 0.25% (w/v) trypsin to digest the cells. When observing the cell morphology under a microscope, we added 5 mL of complete medium to terminate the digestion when the cells

became round. Next, we mixed the cells by gently blowing with a pipette, aspirated all the cells and centrifuged at 1000 rpm for 5 min. Finally, we discarded the supernatant and cultured the cells with a new medium.

### SPDT Apparatus and Protocol

The laser generator (excitation wavelength: 658 nm; Manufacturer: Blueprint Optoelectronics Technology Co., Beijing, China) was used for PDT. The laser radiation intensity was 79.6 mW/cm<sup>2</sup>, and cells were irradiated 63 s. The total dose of laser energy was 5 J/cm<sup>2</sup> (intensity × radiation time). For SDT treatment, 1.0 MHz ultrasound apparatus (WED-100, Welld, Shenzhen, China) was applied to generate ultrasound. The 1 W/cm<sup>2</sup> ultrasound intensity and 1 min treatment time were used in SDT and SPDT treatment groups.

Hepa1-6 cells were seeded in 12-well plates (8 × 10<sup>4</sup> cells/well) and cultured overnight. Cells were divided into six groups: untreated control, PCN224 alone, ultrasound treatment alone, PDT (PCN224 + 5 J/cm<sup>2</sup> laser light), SDT (PCN224 + 1 W/cm<sup>2</sup> ultrasound), and SPDT (PCN224 + 1 W/cm<sup>2</sup> ultrasound + 5 J/cm<sup>2</sup> laser light). Cells in control and ultrasound-alone groups were incubated with serum-free DMEM for 4 h, and cells in the ultrasound-alone group received 1 W/cm<sup>2</sup> ultrasound exposure for 1 min. Cells in other groups were firstly incubated with 10 μg/mL PCN224 in serum-free DMEM for 4 h and then received corresponding treatments. For SPDT treatment, cells were first exposed to ultrasound and then irradiated with 5 J/cm<sup>2</sup> laser light.

### Cytotoxicity Detection

MTT test was used to analyze cytotoxicity. After different treatments, cells in each group were harvested, and 100 μL cell suspension was added to a 96-well plate for another 24 h incubation. After 24 h, viability was determined by adding 10 μL MTT solution (5 mg/mL in PBS) to each well, and the mixture was incubated for additional 4 h at 37 °C in a CO<sub>2</sub> incubator. The nitrogen crystals were dissolved in pure dimethyl sulfoxide, and the absorbance at 570 nm was recorded using the Thermo Scientific Microplate Reader (Multiskan Sky, Thermo Fisher, Waltham, MA, USA, 1510-02362). The cell survival rate was calculated using this equation:

$$\text{Cell survival rate (\%)} = \frac{\text{OD}_{\text{treatment group}}}{\text{OD}_{\text{control group}}} \times 100\%.$$

For the inhibitory experiment, a 7.5 mM concentration of the special ROS scavenger NAC was added to the culture medium when PCN224 was loaded, and the following treatments were the same as in the MTT test.

### Cell Morphology Observation

Hepa1-6 cells were seeded in 12-well plates (8 × 10<sup>4</sup> cells/well) overnight and then subjected to different treatments. After 24 h, the cell morphology in different groups

was observed under an inverted fluorescence microscope (IX73, OLYMPUS, Tokyo, Japan), and the representative cells were amplified.

### *Cell Uptake*

Hepa1-6 cells were seeded in 12-well plates overnight. Then cells were divided into three groups: Control, PCN224, and PCN224 plus ultrasound. The control group was added with serum-free DMEM. The other two groups were added with serum-free DMEM containing 10  $\mu\text{g}/\text{mL}$  PCN224 and incubated for 4 h before cells were harvested. The intracellular PCN224 fluorescence intensity was analyzed by flow cytometry (Accuri® C6 Plus, BD, Franklin Lakes, NJ, USA).

### *Cell Location*

Hepa1-6 cells were inoculated in 24-well plates containing 14 mm diameter coverslips overnight. After being incubated 10  $\mu\text{g}/\text{mL}$  PCN224 for 4 h, cells were washed three times with PBS and then fixed in 4% paraformaldehyde for 10 min. After being washed with PBS, cells were stained with 1  $\mu\text{g}/\text{mL}$  (HO) in PBS at 37 °C for 5 min. The PCN224 red fluorescence and Ho blue fluorescence images were recorded under a forward fluorescence microscope (DP72, OLYMPUS, Tokyo, Japan).

### *Intracellular Reactive Oxygen Species Determination*

The 2',7'-Dichlorofluorescein diacetate (DCFH-DA) was used as a probe to detect the intracellular generation of ROS [18]. Hepa1-6 cells were seeded in 12-well plates ( $8 \times 10^4$  cells/well) overnight, and 4  $\mu\text{M}$  DCFH-DA was added into each well. After 0.5 h of different treatments, cells were harvested and analyzed by flow cytometry (Accuri® C6 Plus, BD, Franklin Lakes, NJ, USA ).

### *Cell Membrane Permeability Analysis*

As a macromolecule, PI can not penetrate the intact cell membrane. When cell membrane permeability increases or is damaged, PI can penetrate into cells and bind to DNA molecules. The intracellular PI fluorescence intensity reflects cell membrane damage [19]. Hepa1-6 cells were seeded in 12-well plates ( $8 \times 10^4$  cells/well) and cultured overnight. PI was added to a cell culture medium treated with SDT, PDT and SPDT for 10 min. At the end, cells were harvested and analyzed by flow cytometry (Accuri® C6 Plus, BD, Franklin Lakes, NJ, USA).

### *DNA Fragmentation Analysis*

According to previous studies, DNA fragmentation can be detected by flow cytometry after adding PI to the cells and permeabilizing them by freeze-thawing [20]. Hepa1-6 cells were seeded in 12-well plates ( $8 \times 10^4$  cells/well) overnight. Instant and subsequent DNA damages were detected after the 0.5 h and 24 h treatments,

and cells in different groups were harvested and washed with PBS. After re-suspension in 200  $\mu\text{L}$  PBS containing 5  $\mu\text{g}/\text{mL}$  PI, the cells were placed in a 1.5 mL Eppendorf tube and immediately transferred into tubes in liquid nitrogen for 30 s and defrosted for 5 min at 37 °C. This process allowed the cells to infiltrate and stain damaged DNA with PI before being analyzed by flow cytometry (Accuri® C6 Plus, BD, Franklin Lakes, NJ, USA).

### *Apoptosis Assay*

Hepa1-6 cells were seeded in 12-well plates ( $8 \times 10^4$  cells/well) overnight and then subjected to SDT, PDT and SPDT treatments. After further incubation for 12 h, all cells were harvested and stained with Annexin V-FITC Apoptosis Detection Kit (C1062, Beyotime Biotechnology, Shanghai, China) according to the manufacturer's instructions. Cell apoptosis was analyzed by flow cytometry (Accuri® C6 Plus, BD, Franklin Lakes, NJ, USA).

### *Mitochondrial Membrane Potential Assay*

Hepa1-6 cells were seeded in 12-well plates ( $8 \times 10^4$  cells/well) overnight and then subjected to SDT, PDT and SPDT treatments. After 0.5 h in different treatments, cells were harvested and resuspended with PBS. After adding 1  $\mu\text{L}$  of the 20  $\mu\text{M}$  stock TMRM reagent solution (20 nM final concentration), the cells were incubated for 30 min at 37 °C and 5% CO<sub>2</sub> and analyzed by flow cytometry (Accuri® C6 Plus, BD, Franklin Lakes, NJ, USA).

### *Cell Microstructure*

The cells were planted on 5 mm diameter cell coverslips overnight and then received different treatments. After 24 h, the cells were washed three times with PBS, and then fixed with 2.5% glutaraldehyde at 4 °C overnight. The cells were dehydrated with 30%, 50%, 70%, 80%, 90%, 95% and 100% ethanol in sequence for 10 min at each gradient. Finally, tert-butyl alcohol was washed three times for 10 min each time. The tert-butyl alcohol was crystallized overnight and freeze-dried. The morphology was observed by scanning transmission electron microscopy.

### *Statistical Analysis*

All data were analyzed and processed mainly with GraphPad Prism 6.0 software (GraphPad Software Inc., San Diego, CA, USA), and data representations in the article are presented as mean  $\pm$  standard deviations (SD). The *t*-test was used for comparisons between two groups, and a one-way analysis of variance was used for comparisons between multiple groups. *p* < 0.05 indicates that the difference is statistically significant.

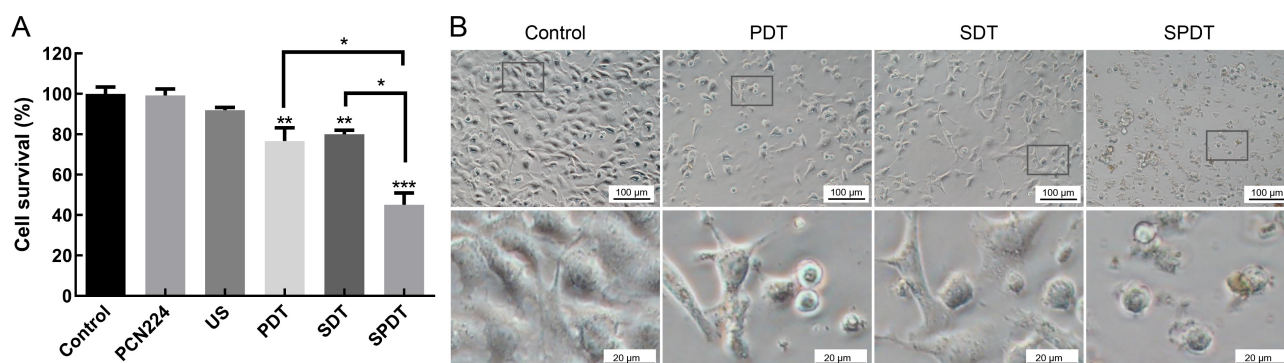


**Fig. 1. Cell viability of Hepa1-6 cells with different treatments.** (A) Control: No treatment; PCN224: 10  $\mu\text{g}/\text{mL}$  PCN224 alone; US: 1  $\text{W}/\text{cm}^2$  ultrasound for 1 min alone; PDT (photodynamic therapy): 10  $\mu\text{g}/\text{mL}$  PCN224 + 5  $\text{J}/\text{cm}^2$  laser light; SDT (sonodynamic therapy): 10  $\mu\text{g}/\text{mL}$  PCN224 + 1  $\text{W}/\text{cm}^2$  ultrasound for 1 min; SPDT (sono-photodynamic therapy): SDT + PDT. All data are expressed as percentages of control; Error bars represent standard deviations of the means from three independent experiments. \* $p < 0.05$ ; \*\* $p < 0.01$  and \*\*\* $p < 0.001$  vs. control group. (B) Cells in different groups were observed under a phase-contrast microscope. Representative images were taken 24 h post-treatment. Scale bar: 100  $\mu\text{m}$  and 20  $\mu\text{m}$ .

## Results

### *PCN224 can be Used as a Novel Sensitizer for SPDT in Hepa1-6 Cells*

PCN224 had been used as photosensitizers in PDT. We first detected Hepa1-6 cytotoxicity after PCN224-SPDT treatment using MTT assays to investigate its potential activity in SPDT. As shown in Fig. 1A, 10  $\mu\text{g}/\text{mL}$  PCN224 or 1.0  $\text{W}/\text{cm}^2$  ultrasound alone treatment did not significantly differ from non-treatment control cells. In contrast, the cell survival rate in SDT group and PDT group were 79.97% and 76.61%, respectively, and all showed significant decreases compared with the control, which implied that PCN224 could be activated by light and ultrasound. Furthermore, the survival rate declined to 45.07% in the SPDT group, showing synergistic cytotoxicity compared with SDT or PDT alone. At the same time, we observed cell morphology using a phase-contrast microscope 24 h after different treatment groups. As seen in Fig. 1B, cell density was reduced compared with the control group, and some cells became shrunk and rounded in both SDT and PDT groups. The cells in the SPDT group showed severe morphological change. Most cells exhibited apoptotic features with severe cell shrinkage, and some cells were fragmented. All the results showed that as a traditional photosensitizer, PCN224 could also be activated by ultrasound. PCN224-SPDT showed an unexpected cytotoxicity effect in Hepa1-6, therefore PCN224 is an excellent sensitizer in SPDT.

### *Cellular Uptake and Distribution of PCN224 in Hepa1-6 Cells*

The accumulation of sensitizers in cells determines the effect of PDT, SDT and SPDT treatments [21]. The cellular PCN224 content was measured by flow cytometry

by analyzing PCN224 fluorescence intensity. As shown in Fig. 2A, compared with the control group, cells in PCN224 treatment group displayed high fluorescence intensity, which indicates the effective absorption of PCN224 by Hepa1-6 cells in our experiment condition. Moreover, 1  $\text{W}/\text{cm}^2$  ultrasound treatment significantly increased the cellular PCN224 content (Fig. 2B), and the improvement of cell membrane permeability after ultrasound treatment may contribute to the accumulation of PCN224 in Hepa1-6 cells. Besides cellular uptake, the distribution of photosensitizers in cells also played an important role in SPDT treatment. As indicated in Fig. 2C, the red fluorescence of PCN224 dispersed throughout the whole cell, including the cell nucleus location (blue fluorescence).

### *Abundant ROS Production Induced by PCN224-SPDT Treatment Played a Key Role in Cell Damage*

This study detected cellular ROS levels after different treatments using ROS probe DCFHDA (2',7'-Dichlorodihydrofluorescein diacetate) combined with flow cytometry. As indicated in Fig. 3A,B, the ROS positive cell rate was 1.0% in the control group, and it increased to 13.6%, 3.9% and 20.6% in PDT, SDT and SPDT treatment groups, respectively.

To further verify the important role of ROS in SPDT-induced cytotoxicity, we used spectral ROS scavenger NAC to eliminate ROS and detect cell viability. Data in Fig. 3C revealed that NAC could relieve cell death in PDT, SDT and SPDT treatment groups. Furthermore, compared with the data in Fig. 1A, the cell survival rate in the SPDT group increased from 45.07% to 83.9%. These results proved that abundant ROS production is an essential factor for anti-tumor effect of PCN224-SPDT treatment.

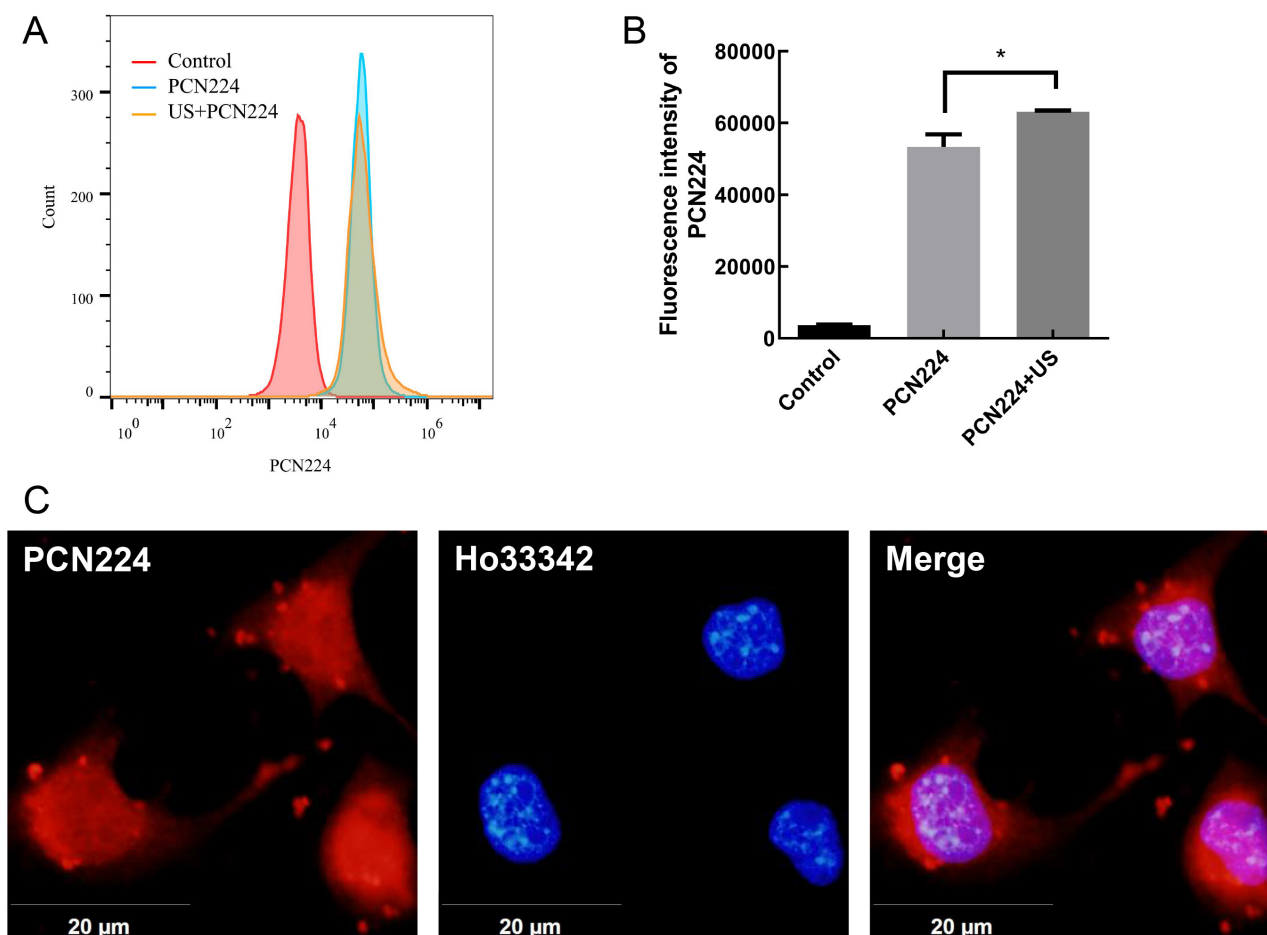


**Fig. 2. Uptake and intracellular localization of PCN224 in Hepa1-6 cells.** (A) Analyze intracellular PCN224 fluorescence intensity after 4 h co-incubation of 10  $\mu\text{g}/\text{mL}$  PCN224 and Hepa1-6 cells with or without ultrasound (1  $\text{W}/\text{cm}^2$ , 1 min) treatments. The control represents cells with no treatment. (B) Quantitative analysis of mean fluorescence intensities of different groups. Data are presented as means  $\pm$  standard deviations from three independent experiments. \* $p < 0.05$ . (C) Hepa1-6 cells were incubated with 10  $\mu\text{g}/\text{mL}$  PCN224 (red channel) for 4 h, and then cells were stained with Ho33342 (HO, nuclear dye, blue channel). After co-loading, cells were visualized by a fluorescence microscope (merge, purple channel).

### *PCN224-SPDT Induced Multisites Damage in Hepa1-6 Cells*

The above results have preliminarily identified that the elevated ROS level in SPDT treatment played a key role in cell damage. According to our results in Fig. 2B, red fluorescence of PCN224 diffused in the whole cells, and PCN224-SPDT may induce multi-site damage. PI is a macromolecule that cannot penetrate the complete cell membrane, and PI staining can be used to detect cell membrane integrity. We stained the cells with PI or not and performed flow cytometry analysis, Fig. 4A–D showed that the PI-positive cells were 5.9%, 8.1% and 24.1% in PDT, SDT and SPDT groups, respectively, at 0.5 h after treatments. The positive cell rate increased to 12.4%, 18.1% and 51.8%, respectively, at 24 h after treatments, and it was significantly higher than the control group.

Fig. 2C showed that PCN224 was also located in the Hepa1-6 cell nucleus. We next detected DNA fragments

by PI staining using flow cytometry after permeabilized PI by freeze-thawing. Fig. 5A–D showed that PI positive cell rates were 6.9%, 7.1% and 11.8% ( $p < 0.001$ ) in PDT, SDT and SPDT groups, respectively, at 0.5 h after treatments, and the positive cell rate increased to 11.2%, 18.3% and 44.0% 24 h after different treatments. All showed a significant increase compared with the control group. These results implied that DNA damage caused by PCN224-SPDT was difficult to be repaired through a cellular repair system and caused serious cell death.

Mitochondrial membrane potential (MMP) decrease was a vital hallmark for mitochondrial damage. Therefore, we detected the MMP of Hepa1-6 cells with different treatments to analyze the mitochondrial injury. As we can see in Fig. 6A,B, 0.5 h after PDT, SDT and SPDT treatments, 7.4%, 10.8% and 19.9% cells showed lower MMP, respectively. These preliminary results proved that PCN224-SPDT induced damage to mitochondria.

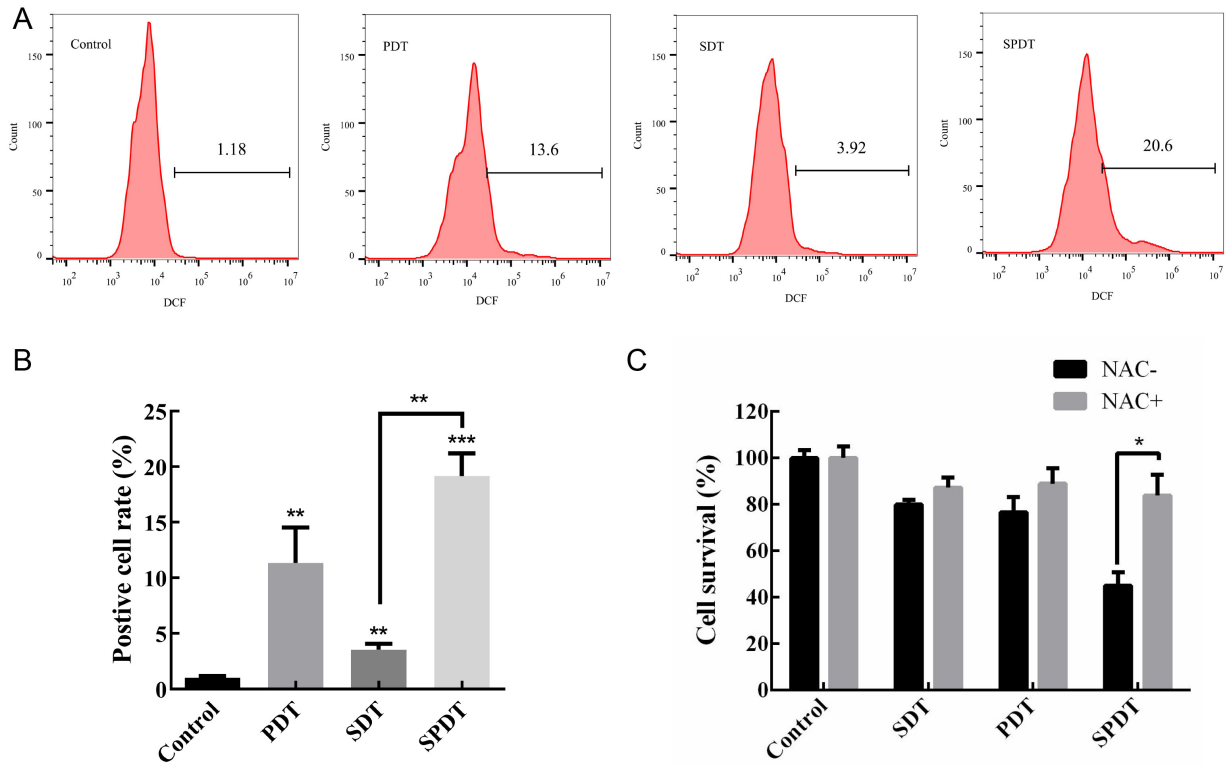


**Fig. 3. Intracellular ROS measurement.** (A) DCFH-DA was used to detect intracellular ROS production 0.5 h after different treatments. Cells with DCF fluorescence were analyzed with flow cytometry. (B) Quantification of ROS production in Hepa1-6 cells (n = 3). \**p* < 0.05; \*\**p* < 0.01 and \*\*\**p* < 0.001 vs. control group. (C) Effect of the reactive oxygen species scavenger Nacetylcysteine (NAC) on SPDT-induced cytotoxicity in Hepa1-6 cells. \**p* < 0.05 between the same group with or without NAC.

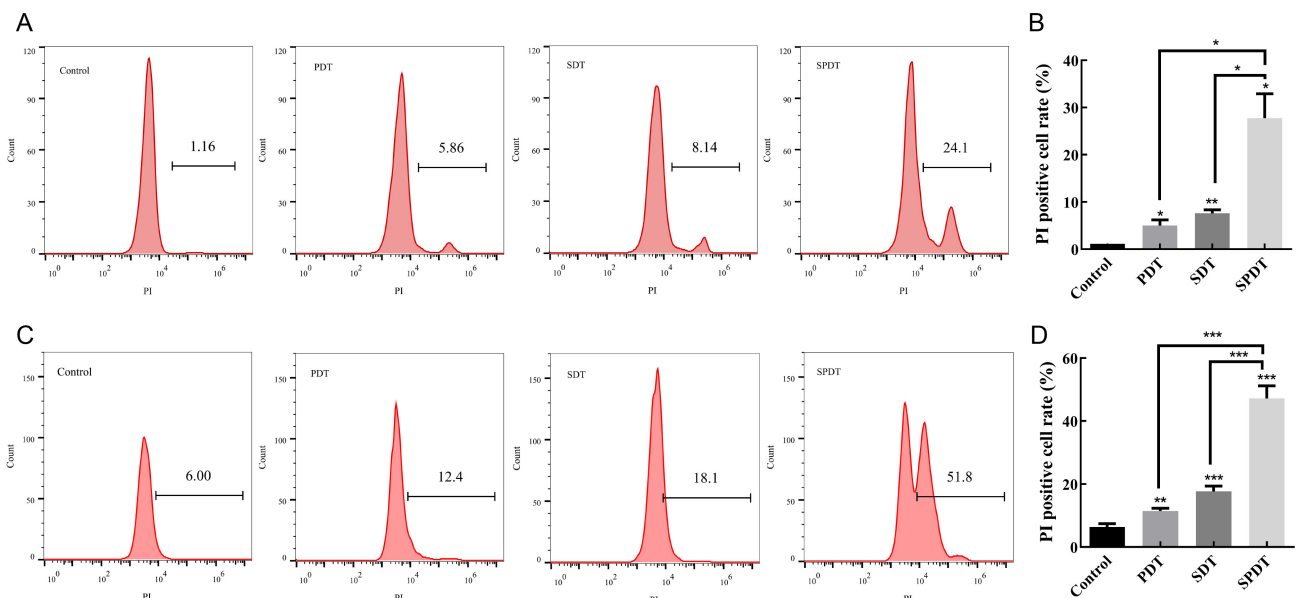


**Fig. 4. Cell membrane permeability detection.** Flow cytometric analysis showing PI uptake by Hepa1-6 cells treated with different treatments. (A) At 0.5 h after different treatments, Hepa1-6 cells were stained with PI, and PI-positive cells were analyzed by flow cytometry. (B) Quantification of PI-positive cells in different treatments 0.5 h after treatments (n = 3). (C) At 24 h after treatments, Hepa1-6 cells were stained with PI and PI-positive cells were detected by flow cytometry. (D) Quantification of PI-positive cells in different treatments 24 h after treatments (n = 3). \**p* < 0.05, \*\**p* < 0.01 and \*\*\**p* < 0.001 versus control and between groups.

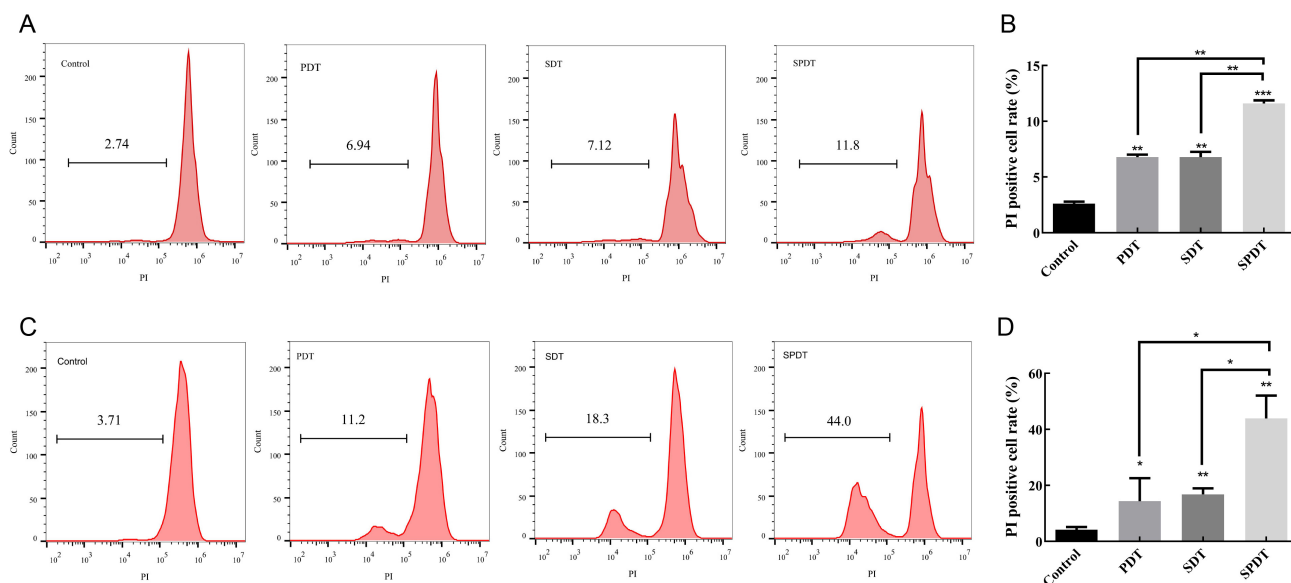


**Fig. 5. Analysis of DNA fragmentation.** (A) DNA fragmentation analysis at 0.5 h after different treatments by flow cytometry. (B) Quantification analysis of DNA fragmentation rate after different treatments (n = 3). (C) DNA fragmentation analysis at 24 h after different treatments by flow cytometry (n = 3). (D) Quantification analysis of DNA fragmentation rate after 24 h different treatments (n = 3). \* $p < 0.05$ , \*\* $p < 0.01$  and \*\*\* $p < 0.001$  versus control and between groups.

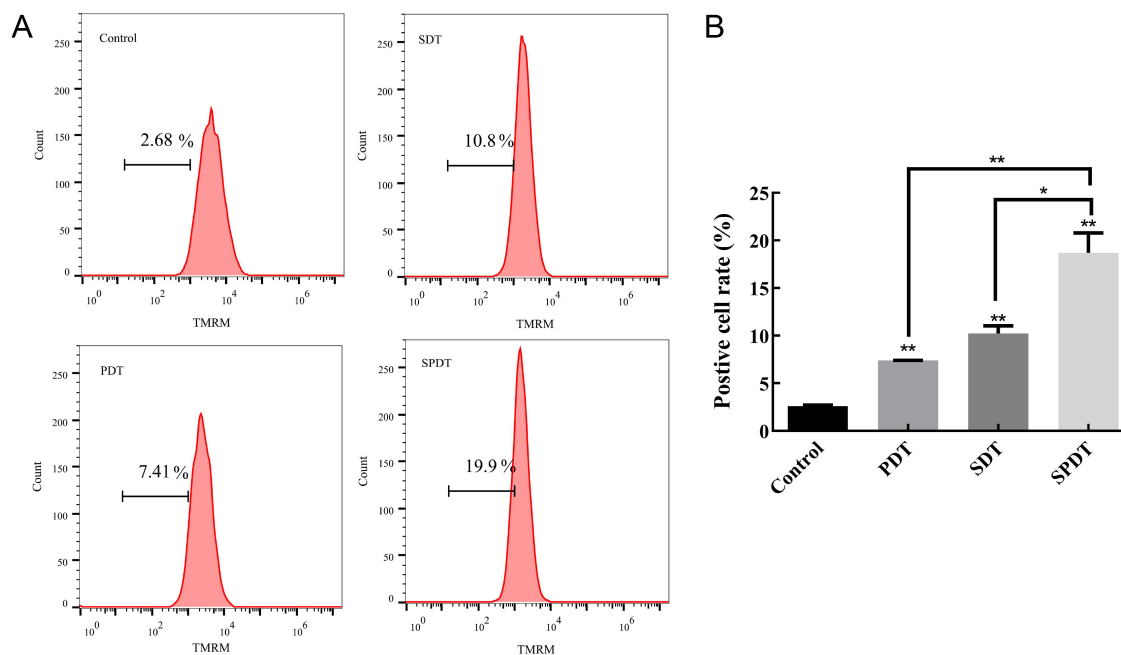


**Fig. 6. Detection of the mitochondrial membrane potential of Hepa1-6 cells after treatments.** (A) At 0.5 h after treatments, cells were stained with TMRM and detected by flow cytometry. (B) Quantification analysis of MMP decreased cell rate in different treatments (n = 3). \* $p < 0.05$  and \*\* $p < 0.01$ .

### Cell Apoptosis and Ultrastructural Detection

We next detected cell apoptosis levels induced by PCN224-SPDT treatment. Fig. 7A,B showed that cell apoptosis rates were 19.8%, 15.1% and 29.3% in PDT, SDT and SPDT groups at 24 h after treatment. The SPDT treatment significantly increased cell apoptosis rate com-

pared with PDT and SDT treatment ( $p < 0.01$ ). To further identify the state of cell death induced by SPDT treatment, we used a scanning electron microscope to observe cellular ultrastructural (Fig. 8). Compared with negative control cells, remarkable shrinkage and cell membrane depression were observed after PDT and SDT treatments. The SPDT-

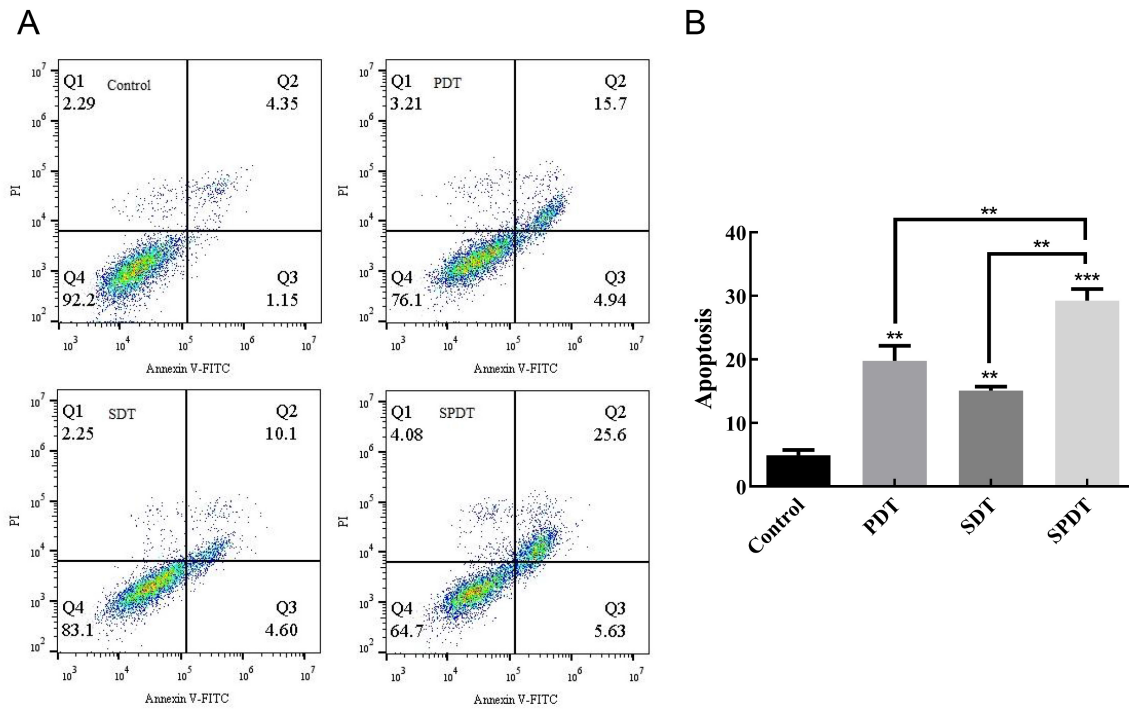


**Fig. 7. Apoptosis assay.** (A) Apoptotic populations of Hepal-6 cells as a result of different treatments analyzed by Annexin V/PI double staining method. (B) Total apoptosis rate (%) of Hepal-6 cells after different treatments (n = 3). \*\* $p < 0.01$  and \*\*\* $p < 0.001$  versus control and between groups.

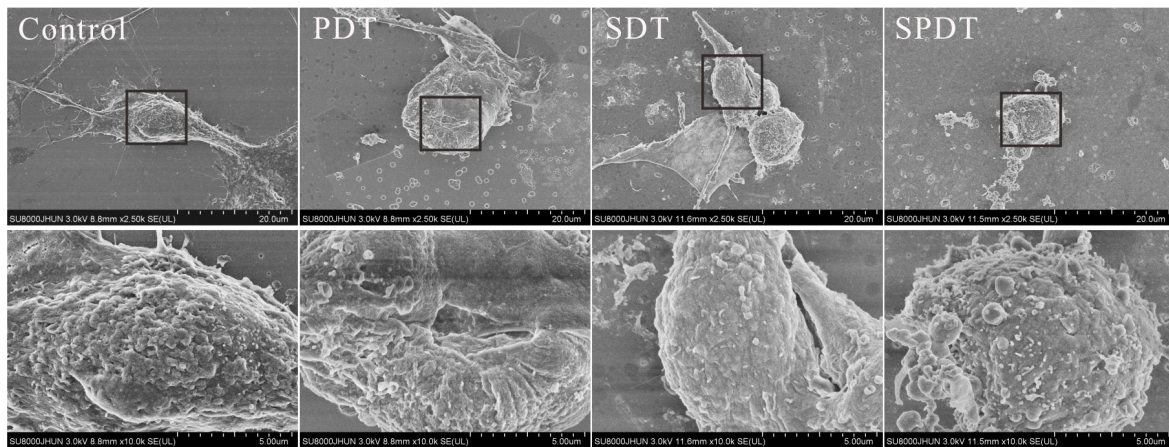


**Fig. 8. The microstructure of cells after 24 h different treatments by scanning transmission electron microscopy.** Scale bar: 20  $\mu\text{m}$ , 5  $\mu\text{m}$ .

treated cells displayed significant shrinking with cell size decreased to about 10  $\mu\text{m}$ , and microvilli disappeared with the appearance of apoptotic bodies. PCN224-SPDT can induce Hepal-6 cell apoptosis.

## Discussion

This study revealed that PCN224 could be used as a novel sensitizer in SPDT treatment, and PCN224-SPDT could cause severe cytotoxicity at low PCN224 concentrations and low light or low ultrasound intensities. In addition,

PCN224-SPDT could induce multisite damage, cell membrane damage, mitochondrial damage, and DNA damage, leading to apoptosis and attributing to the total intracellular distribution of ROS and the overall distribution of PCN224 in the cell.

The cell distribution of PCN224 was different from other monomer photosensitizers, such as chlorophyllin e6 and DVDMS (sinoporphyrin sodium), which are mainly located in the cell mitochondria [22,23]. The difference in intracellular distribution may be related to the difference in properties between pure compounds and MOF. There-

fore, the widespread distribution of PCN224 in Hepa1-6 cells may contribute to the effective cytotoxicity of SDT, PDT and SPDT. Excessive cytotoxic ROS production during SPDT is an essential mechanism for killing tumor cells [24]. Furthermore, a large amount of ROS in the SPDT process can oxidize various biological macromolecules and important enzymes in tumor cells, thus inducing tumor cell death [25]. Our results show that ROS production is a key factor in the anti-tumor effect of PCN224-SPDT treatment.

ROS includes singlet oxygen, superoxide anion and hydroxyl radical, and these species have a very short lifetime (about 10–300 ns) and tight diffusion (about 10–50 nm) in cells [26]. Therefore, the ROS only induces damage around the generation site. In addition, the abundance of ROS in PCN224-SPDT and ultrasonic vaporization [27] may lead to immediate cell membrane damage and subsequent cellular responses leading to more severe cell membrane damage. Mitochondria are sensitive to external stimuli and are susceptible to oxidation, which ultimately leads to mitochondria-dependent apoptosis [28,29]. Meanwhile, apoptosis is a programmed type of cell death regulated by endogenous or exogenous signaling pathways. Mitochondrial or DNA damage is the main trigger for the induction of apoptosis [30]. In conclusion, these studies support our results that PCN224-SPDT exerts anti-tumor effects by promoting ROS production to induce mitochondrial damage and DNA damage, leading to apoptosis.

## Conclusions

Our results demonstrate that PCN224 can be used as a novel sensitizer in SPDT treatment. PCN224-SPDT shows excellent cytotoxicity in Hepa1-6 cells, and PCN224 is located in the whole Hepa1-6 cells to induce multi-site injury via oxidative stress from ROS production under PCN224-SPDT treatment. The wide cell damage ultimately results in cell apoptosis.

## Availability of Data and Materials

The data used to support the findings of this study are available from the corresponding author upon request.

## Author Contributions

BLS and KHH—designed the research study; JSC, HPW and FY—performed the research; QP and WLL—provided help and advice on the flow cytometry experiments; HPW and JSC—analyzed the data and wrote the manuscript. All authors contributed to editorial changes in the manuscript. All authors read and approved the final manuscript. All authors have participated sufficiently in the work and agreed to be accountable for all aspects of the work.

## Ethics Approval and Consent to Participate

Not applicable.

## Funding

This work was supported by the Natural Science Foundation of Hubei Province, China (2020CFB448), the Health Commission of Hubei Province Scientific Research Project (WJ2021M216), the Key R&D Project of Hubei Province (Social Development) China (2022BCA018), the scientific research start-up funds of Jiangnan University (1010/08500003, 1010/08190001).

## Acknowledgment

Not applicable.

## Conflict of Interest

The authors declare no conflict of interest.

## Appendix

See Fig. 8.

## References

- [1] Dinakaran D, Sengupta J, Pink D, *et al.* PEG-PLGA nanospheres loaded with nanoscintillators and photosensitizers for radiation-activated photodynamic therapy. *Acta Biomater.* 2020;117:335–348. doi: [10.1016/j.actbio.2020.09.029](https://doi.org/10.1016/j.actbio.2020.09.029)
- [2] Rajora MA, Lou JWH, Zheng G. Advancing porphyrin's biomedical utility via supramolecular chemistry. *Chem Soc Rev.* 2017;46(21):6433–6469. doi: [10.1039/c7cs00525c](https://doi.org/10.1039/c7cs00525c)
- [3] Fraix A, Sortino S. Combination of PDT photosensitizers with NO photodonors. *Photochem Photobiol Sci.* 2018;17(11):1709–1727. doi: [10.1039/c8pp00272j](https://doi.org/10.1039/c8pp00272j)
- [4] Zhang Y, Du X, Liu S, *et al.* NIR-triggerable ROS-responsive cluster-bomb-like nanoplatfor for enhanced tumor penetration, phototherapy efficiency and antitumor immunity. *Biomaterials.* 2021;278:121135. doi: [10.1016/j.biomaterials.2021.121135](https://doi.org/10.1016/j.biomaterials.2021.121135)
- [5] Wang L, Zhang Y, Han Y, *et al.* Nanoscale photosensitizer with tumor-selective turn-on fluorescence and activatable photodynamic therapy treatment for COX-2 overexpressed cancer cells. *J Mater Chem B.* 2021;9(8):2001–2009. doi: [10.1039/d0tb02828b](https://doi.org/10.1039/d0tb02828b)
- [6] Huang Y, Guan Z, Dai X, *et al.* Engineered macrophages as near-infrared light activated drug vectors for chemo-photodynamic therapy of primary and bone metastatic breast cancer. *Nat Commun.* 2021;12(1):4310. doi: [10.1038/s41467-021-24564-0](https://doi.org/10.1038/s41467-021-24564-0)
- [7] Teh DBL, Bansal A, Chai C, *et al.* A Flexi-PEGDA Upconversion Implant for Wireless Brain Photodynamic Therapy. *Adv Mater.* 2020;32(29):e2001459. doi: [10.1002/adma.202001459](https://doi.org/10.1002/adma.202001459)
- [8] Honari A, Merillat DA, Bellary A, Ghaderi M, Sirsi SR. Improving Release of Liposome-Encapsulated Drugs with Focused Ultrasound and Vaporizable Droplet-Liposome Nanoclusters. *Pharmaceutics.* 2021;13(5):609. doi: [10.3390/pharmaceutics13050609](https://doi.org/10.3390/pharmaceutics13050609)
- [9] May JN, Golombek SK, Baues M, *et al.* Multimodal and multiscale optical imaging of nanomedicine delivery across

- the blood-brain barrier upon sonopermeation. *Theranostics*. 2020;10(4):1948–1959. doi: [10.7150/thno.41161](https://doi.org/10.7150/thno.41161)
- [10] Giuntini F, Foglietta F, Marucco AM, *et al.* Insight into ultrasound-mediated reactive oxygen species generation by various metal-porphyrin complexes. *Free Radic Biol Med*. 2018;121:190–201. doi: [10.1016/j.freeradbiomed.2018.05.002](https://doi.org/10.1016/j.freeradbiomed.2018.05.002)
- [11] Zhu J, Wang Y, Yang P, *et al.* GPC3-targeted and curcumin-loaded phospholipid microbubbles for sono-photodynamic therapy in liver cancer cells. *Colloids Surf B Biointerfaces*. 2021;197:111358. doi: [10.1016/j.colsurfb.2020.111358](https://doi.org/10.1016/j.colsurfb.2020.111358)
- [12] Glueck M, Hamminger C, Fefer M, Liu J, Plaetzer K. Save the crop: Photodynamic Inactivation of plant pathogens I: bacteria. *Photochem Photobiol Sci*. 2019;18(7):1700–1708. doi: [10.1039/c9pp00128j](https://doi.org/10.1039/c9pp00128j)
- [13] Lin N, Li C, Wang Z, *et al.* A safety study of a novel photosensitizer, sinoporphyrin sodium, for photodynamic therapy in Beagle dogs. *Photochem Photobiol Sci*. 2015;14(4):815–832. doi: [10.1039/c4pp00463a](https://doi.org/10.1039/c4pp00463a)
- [14] Tamiaki H, Fukai K, Nakamura S. Intramolecular interaction of synthetic chlorophyll heterodyads with different  $\pi$ -skeletons. *Photochem Photobiol Sci*. 2020;19(3):332–340. doi: [10.1039/c9pp00373h](https://doi.org/10.1039/c9pp00373h)
- [15] Okada K, Tanaka Y, Inose T, Ujii H, Yoshikawa H, Tanaka D. Electrolytic synthesis of porphyrinic Zr-metal-organic frameworks with selective crystal topologies. *Dalton Trans*. 2021;50(16):5411–5415. doi: [10.1039/d1dt00491c](https://doi.org/10.1039/d1dt00491c)
- [16] Kim K, Lee S, Jin E, *et al.* MOF  $\times$  Biopolymer: Collaborative Combination of Metal-Organic Framework and Biopolymer for Advanced Anticancer Therapy. *ACS Appl Mater Interfaces*. 2019;11(31):27512–27520. doi: [10.1021/acsami.9b05736](https://doi.org/10.1021/acsami.9b05736)
- [17] Chen LJ, Liu YY, Zhao X, Yan XP. Vancomycin-Functionalized Porphyrinic Metal-Organic Framework PCN-224 with Enhanced Antibacterial Activity against *Staphylococcus Aureus*. *Chem Asian J*. 2021;16(15):2022–2026. doi: [10.1002/asia.202100546](https://doi.org/10.1002/asia.202100546)
- [18] Won M, Koo S, Li H, *et al.* An Ethacrynic Acid-Brominated BODIPY Photosensitizer (EA-BPS) Construct Enhances the Lethality of Reactive Oxygen Species in Hypoxic Tumor-Targeted Photodynamic Therapy. *Angew Chem Int Ed Engl*. 2021;60(6):3196–3204. doi: [10.1002/anie.202012687](https://doi.org/10.1002/anie.202012687)
- [19] Chen R, Zhu Q, Fang Z, *et al.* Aluminum induces oxidative damage in *Saccharomyces cerevisiae*. *Can J Microbiol*. 2020;66(12):713–722. doi: [10.1139/cjm-2020-0084](https://doi.org/10.1139/cjm-2020-0084)
- [20] Shojaeian K, Nouri H, Kohram H. Does MnTBAP ameliorate DNA fragmentation and *in vivo* fertility of frozen-thawed Arabian stallion sperm?. *Theriogenology*. 2018;108:16–21. doi: [10.1016/j.theriogenology.2017.11.019](https://doi.org/10.1016/j.theriogenology.2017.11.019)
- [21] Jockusch S, Kräutler B. The red chlorophyll catabolite (RCC) is an inefficient sensitizer of singlet oxygen - photochemical studies of the methyl ester of RCC. *Photochem Photobiol Sci*. 2020;19(5):668–673. doi: [10.1039/d0pp00071j](https://doi.org/10.1039/d0pp00071j)
- [22] Shinoda Y, Kujirai K, Aoki K, *et al.* Novel Photosensitizer  $\beta$ -Mannose-Conjugated Chlorin e6 as a Potent Anticancer Agent for Human Glioblastoma U251 Cells. *Pharmaceuticals (Basel)*. 2020;13(10):316. doi: [10.3390/ph13100316](https://doi.org/10.3390/ph13100316)
- [23] Shen Y, Chen Y, Huang Y, *et al.* An *in vitro* study on the antitumor effect of sonodynamic therapy using sinoporphyrin sodium on human glioblastoma cells. *Ultrasonics*. 2021;110:106272. doi: [10.1016/j.ultras.2020.106272](https://doi.org/10.1016/j.ultras.2020.106272)
- [24] Galadari S, Rahman A, Pallichankandy S, Thayyullathil F. Reactive oxygen species and cancer paradox: To promote or to suppress? *Free Radic Biol Med*. 2017;104:144–164. doi: [10.1016/j.freeradbiomed.2017.01.004](https://doi.org/10.1016/j.freeradbiomed.2017.01.004)
- [25] Droste A, Chaves G, Stein S, *et al.* Zinc accelerates respiratory burst termination in human PMN. *Redox Biol*. 2021;47:102133. doi: [10.1016/j.redox.2021.102133](https://doi.org/10.1016/j.redox.2021.102133)
- [26] Jaganjac M, Cipak A, Schaur RJ, Zarkovic N. Pathophysiology of neutrophil-mediated extracellular redox reactions. *Front Biosci (Landmark Ed)*. 2016;21(4):839–855. doi: [10.2741/4423](https://doi.org/10.2741/4423)
- [27] Haugse R, Langer A, Murvold ET, *et al.* Low-Intensity Sonoporation-Induced Intracellular Signalling of Pancreatic Cancer Cells, Fibroblasts and Endothelial Cells. *Pharmaceutics*. 2020;12(11):1058. doi: [10.3390/pharmaceutics12111058](https://doi.org/10.3390/pharmaceutics12111058)
- [28] Zhu H, Toan S, Mui D, Zhou H. Mitochondrial quality surveillance as a therapeutic target in myocardial infarction. *Acta Physiol (Oxf)*. 2021;231(3):e13590. doi: [10.1111/apha.13590](https://doi.org/10.1111/apha.13590)
- [29] Jiao H, Jiang D, Hu X, *et al.* Mitocytosis, a migrasome-mediated mitochondrial quality-control process. *Cell*. 2021;184(11):2896–2910.e13. doi: [10.1016/j.cell.2021.04.027](https://doi.org/10.1016/j.cell.2021.04.027)
- [30] Suehiro S, Ohnishi T, Yamashita D, *et al.* Enhancement of antitumor activity by using 5-ALA-mediated sonodynamic therapy to induce apoptosis in malignant gliomas: significance of high-intensity focused ultrasound on 5-ALA-SDT in a mouse glioma model. *J Neurosurg*. 2018;129(6):1416–1428. doi: [10.3171/2017.6.JNS162398](https://doi.org/10.3171/2017.6.JNS162398)